Rare Metal Materials and Engineering
Available online at **www.rmme.ac.cn**

Cite this article as: Rare Metal Materials and Engineering.

DOI: 10.12442/j.issn.1002-185X.E20230047

Development of ultra-coarse grained WC-8(Co,Ni) cemented carbides with varied Ni:Co ratios leveraging thermodynamic phase diagram calculations

Zhiwei Shang [1], Zhiping Sun [1, 2], Zhiming Wang [1, 2] Wenkai Zhao [1], Yaning Chen [1]

[1] School of Mechanical Engineering, Qilu University of Technology (Shandong Academy of Sciences), Ji'nan 250353, China; [2] Shandong Institute of Mechanical Design and Research, Ji'nan 250353, China

Abstract: This study is grounded in thermodynamic phase diagram calculations and employs powder metallurgy techniques to fabricate ultra-coarse grained WC-8(Co,Ni) cemented carbides with varying Ni:Co ratios. The study delves into the alloy's microscopic structure, mechanical properties and corrosion resistance. It has been shown that carbon equilibrium can be efficiently maintained by using thermodynamic phase diagram calculations, thus preventing the emergence of harmful phases associated with carbon deficiency or excess in the alloy. As the Ni:Co ratio increases, the density of the alloy first increases and then decreases. The average grain size of WC enlarges, leading to a deterioration in the uniformity of the binder phase distribution. This results in a decrease in hardness, an increase in fracture toughness, and an initial rise followed by a significant decrease in flexural strength. Ni plays a crucial role in mitigating the corrosion rate of the binder phase and thus enhancing the corrosion resistance of ultra-coarse grained cemented carbides. When the Ni:Co ratio is 2:6, the alloy demonstrates optimal integrated mechanical properties and its enhanced corrosion resistance is notably pronounced.

Keywords: Ultra-coarse cemented carbides; Ni addition; Phase diagram; Properties; Corrosion resistance

WC-Co cemented carbides consist of WC as the hard phase and Co as the binding phase and are synthesized by powder metallurgical sintering[1-2]. Due to their simple composition and excellent performance, they are widely used in applications such as cutting tools and drilling equipment[3]. Ultra-coarse WC-Co cemented carbides, characterized by large WC grain size and thick Co layers, have become a focal point of current research in the engineering field due to their excellent fracture toughness and resistance to thermal shock[4]. During constrution in environments with a high concentration of chloride ions, the alloy is highly susceptible to electrochemical corrosion. The thicker Co layers at the grain boundaries, with their lower standard electrode potential, tend to act as anode in the corrosion cell and undergo oxidation reactions leading to dissolution. This, in turn, weakens the bonds between WC grains and results in detachment and porosity[5]. Therefore, corrosion resistance plays a crucial role in enabling the engineering applications of ultra-coarse cemented carbides.

Corrosion of cemented carbides generally occurs in the binder phase, while the hard phase is protected due to its higher standard electrode potential[6]. It has been shown that the incorporation of a suitable amount of the corrosionresistant metal elements into the cemented carbide binder phase significantly improves the corrosion resistance of the alloy[7-8]. Ni and Co exhibit closely aligned physical and chemical properties, along with unique passivation and oxidation resistance characteristics. Ni are frequently used in place of the binder component Co, with the goal of improving the corrosion resistance of the alloy. However, Ni also possesses a

Foundation item:Natural Science Foundation of Shandong Province (ZR2021ME023)
Corresponding author:Zhiping Sun, Ph.D., Associate Professor, School of Mechanical Engineering, Qilu University of Technology (Shandong Academy of Sciences), Jinan 250353, P. R. China,Tel: +86 18353108673, E-mail: Benzsun@163.com

higher stacking fault energy and lower work-hardening capability, which prevents its complete substitution for Co as a binding agent[9]. The addition of an appropriate amount of Ni to the binder phase is crucial for the synergistic enhancement of the mechanical and corrosion resistance properties of ultra-coarse WC-8(Co,Ni) cemented carbides. Current research has placed limited emphasis on the influence of different Ni:Co ratios on the mechanical properties of ultra-coarse WC-(Co, Ni) cemented carbides, especially concerning corrosion behavior in chloride ion-enriched environments, which remains insufficiently explored[10].

This study designs ultra-coarse WC-8(Co,Ni) cemented carbides with varying Ni:Co ratios in the binder phase. It employs thermodynamic phase diagram calculations to control carbon equilibration and uses powder metallurgy techniques for alloy fabrication. The study examines and analyzes the microstructure and mechanical properties of the alloys to determine the optimal Ni:Co ratio for achieving the best overall performance. In addition, this study investigates the behavior of corrosion in a simulated high-chloride environment resembling seawater, providing theoretical support for the practical application of ultra-coarse cemented carbides in engineering.

1 Experiment

1.1 Thermodynamic Calculation Phase Diagram

In the binder phase, the solubility of W in Ni significantly exceeds that of C. This disparity often poses challenges in maintaining consistent carbon content during sintering, potentially leading to the manifestation of the carbon-deficient η-phase and the carbon-rich graphite phase[11]. To address this, we utilized thermodynamic phase diagram calculations via the Thermo-Calc software 2022a (*Database - TCCC1: cemented carbides v1.0*) to ensure carbon equilibrium. Fig. 1 illustrates the thermodynamic phase diagram calculations for various Ni:Co ratios, with blue boxes indicating the carbon window range and black dotted line indicating the selected experimental carbon content. The carbon content of the base powder is adjusted during the blending phase to ensure the desired carbon balance.

1.2 Materials and methods

The composition of the alloy in the following ratios: WC-8Co (N00), WC-6Co-2Ni (N02), WC-4Co-4Ni (N04)，WC-2Co-6Ni (N06). Fig. 2 outlines the alloy preparation process. The preparation method employed in this study follows the powder metallurgy approach, encompassing grinding, drying, pressing, and vacuum sintering. As depicted in Fig. 2a, coarse WC powder (25μm), fine WC powder (1μm), Co powder (2μm), and Ni powder (1.5μm) were initially weighed according to the mass ratios outlined in Table 1. These components were then placed in anhydrous ethanol and subjected to one hour of ultrasonic vibration to generate the raw material solution. Similarly, polyethylene glycol (PEG-4000) was used to create a binder solution. Following this, the binder solution is mixed with the raw material solution and subjected to ultrasonic vibration for one hour to form a slurry. The slurry is poured into stainless steel ball mill jars. In order to minimize the breakage of a substantial number of coarse WC particles and to achieve comprehensive mixing, the spherical milling parameter was set to 63 rpm for wet milling over a 16-hour period, as depicted in Fig. 2b. After milling, the slurry was dried and sifted, followed by uniaxial pressing at 120 MPa using a single punch press. Subsequently, the samples were subjected to vacuum sintering, as illustrated by the sintering curve in Fig. 2c. In order to minimize the Co and Ni volatilization during the sintering process and to enhance the alloy density, an Ar gas is introduced during vacuum sintering, as indicated in Fig. 2d.

1.3 Material characterizations

The relative densities of the samples were calculated using the Archimedean principle and mixing theory. Hardness was tested using a Vickers hardness tester (HTV-PHS30) with a 30kg (HV_{30}) load. Fracture toughness was determined using the single-edge notched beam (SENB) method. The alloy's flexural strength was measured using a three-point bending test on an electronic universal testing machine (AGS-X5KN) with a loading rate of 0.5 mm/min and an 18 mm span. The microstructure, fracture morphology, and the microscopic structure of the corroded samples were observed using a scanning electron microscope (SU3500) equipped with an energy-dispersive X-ray spectroscopy (EDS) analyzer (Quantax400). The WC grain size of the alloy was measured using a linear truncation method. Phase composition analysis of the samples was conducted using an X-ray diffractometer (D8-ADVANCE).

Electrochemical corrosion experiments were performed using a Gamry Interface 1000 electrochemical workstation in a three-electrode system. The samples served as the working electrode, a saturated calomel electrode (SCE) was used as the reference electrode, and a platinum electrode served as the counter electrode (CE). Prior to testing, the sample surfaces were polished to a roughness below 1μm, followed by ultrasonic cleaning. The corrosion solution was a 3.6 wt.% NaCl solution with a pH of 7, simulating seawater conditions. The electrochemical corrosion polarization curves (Tafel) were obtained by testing within a potential range of ±0.8 V at a scan rate of 5

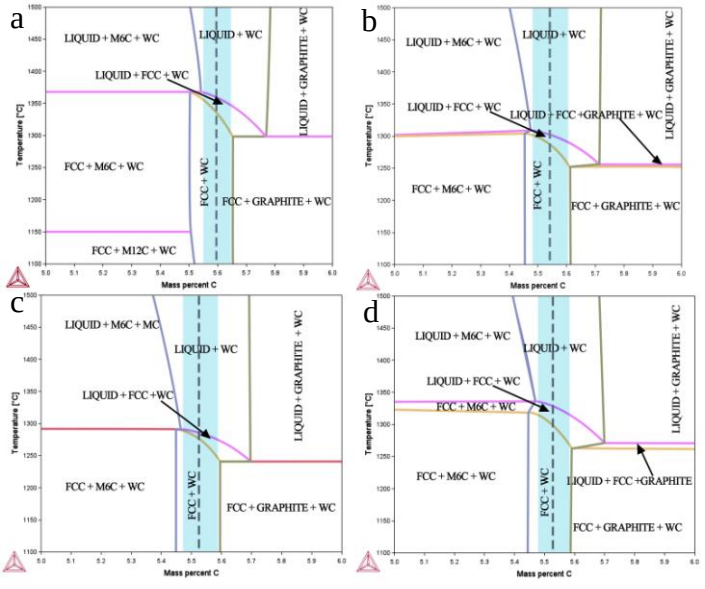

Fig.1 Thermodynamic calculation phase diagram of ultra-coarse WC-8(Co,Ni) cemented carbide (a) Ni:Co = 0:8 (b) Ni:Co = 2:6 (c) Ni:Co = 4:4 (d) Ni:Co = 6:2

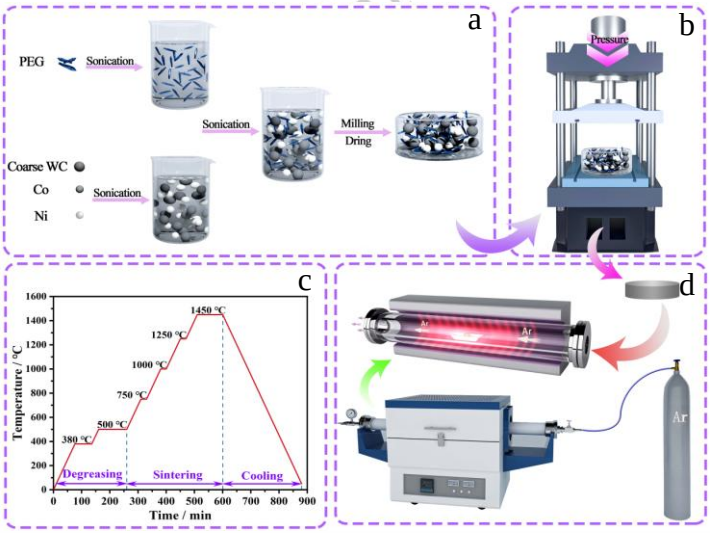

Fig.2 (a) Powder mixing process (b) Pressing process (c) Sintering temperature curves (d) Vacuum sintering process

2 Results and Discussion

2.1 Composition and microstructure

Fig. 3 shows XRD pattern of ultra-coarse WC-8(Co,Ni) cemented carbides with different Ni:Co ratios. As observed in the graph, the alloy phases consist of the typical WC phase and the γ-binder phase, with no detection of other detrimental phases such as the carbon-deficient η-phase or the carbon-rich graphite phase[12]. This suggests that efficient control of the alloy carbon balance can be achieved using thermodynamic calculations and timely carbon replenishment during preparation. As the Ni:Co ratio increases, the diffraction peak intensity of the binder phase gradually strengthens and shifts toward larger angles. This suggests a reduction in the lattice constants of the Co-Ni solid solution phase (with Co having an atomic radius 0.043 nm larger than Ni). The solid solution strengthening mechanism due to Ni dissolving into Co is weakened, which may adversely affect the mechanical properties of the alloy[13].

Fig. 4 shows SEM images of ultra-coarse WC-8(Co,Ni) cemented carbides with varying Ni:Co ratios. These alloys consist of gray regions representing the WC phase and black regions indicating the γ binder phase. The average WC grain size falls within the range of 5μm-8μm, aligning with the definition of ultra-coarse cemented carbide alloys[14]. As the Ni:Co ratio increases, the average WC grain size transitions from 5.51μm to 6.28μm. This phenomenon is attributed to the greater solubility of WC in Ni compared to Co. Consequently, under the same sintering temperature, a higher Ni content in the binder phase results in an increased quantity of precipitated liquid phase, subsequently leading to faster grain recrystallization during cooling[15].From Fig. 4a, it is evident that the N00 alloy exhibits a relatively uniform distribution of WC grains and Co phases, with no significant difference in the thickness of the Co phase and no significant defects such as pores or cracks. Since WC belongs to the hexagonal non-equiaxial crystalline system, it exhibits orientational behavior during liquid-phase sintering, often resulting in triangular or irregularly shaped grains[16]. However, Fig. 4d reveals that the WC grain boundaries become less distinct, the uniformity of the Co-Ni binder phase distribution deteriorates, and exceptionally large grains emerge. This can be attributed to Ni raising the temperature of the eutectic reaction in the alloy, which shortens the liquid-phase sintering time. In addition, Ni exhibits poorer wetting properties with WC compared to Co. Thus, during liquid-phase sintering, the liquid phase spreads less uniformly over the WC grain surface, resulting in non-uniform diffusion.

Fig. 5 illustrates the relative densities of ultra-coarse WC-8(Co,Ni) cemented carbides with different Ni:Co ratios. Due to the favorable wettability exhibited by both Co and Ni toward WC particles, and aided by the enhanced sintering effect of low-pressure argon gas, the densification of all samples exceeded 98%. With an increase in the Ni:Co ratio, the relative density of the alloy initially experiences a slight increase before decreasing. When the Ni:Co ratio reaches 2:6, the N02 alloy shows the highest relative density at 99.33%. The densification of ultra-coarse cemented carbides relies on the rearrangement of WC particles, the diffusion of the binder phase, and its viscous flow. Since Ni has a greater solubility in WC than Co, the increased Ni content in the composite binder phase leads to an increase in the quantity of the liquid phase, promoting the viscous flow of the liquid phase and the dissolution-precipitation process of WC grains, thereby contributing to the densification of the alloy[17]. However, due to the lower wetting ability of Ni compared to Co, the flow resistance of WC particles during liquid-phase sintering increases when the Ni:Co ratio reaches 4:4, limiting the rearrangement process and causing defects such as pores and microcracks. At this point, the advantage of Ni's solubility in promoting densification is offset by the deterioration of wetting properties, leading to a decrease in the alloy's relative density.

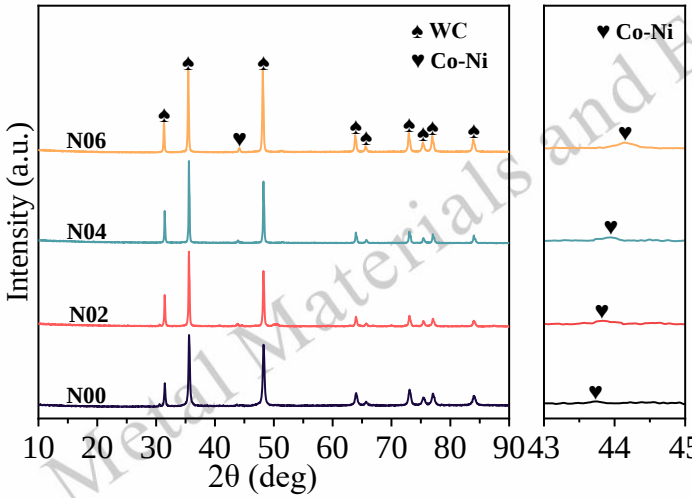

Fig.3 XRD pattern of ultra-coarse WC-8(Co,Ni) cemented carbides with different Ni:Co ratios

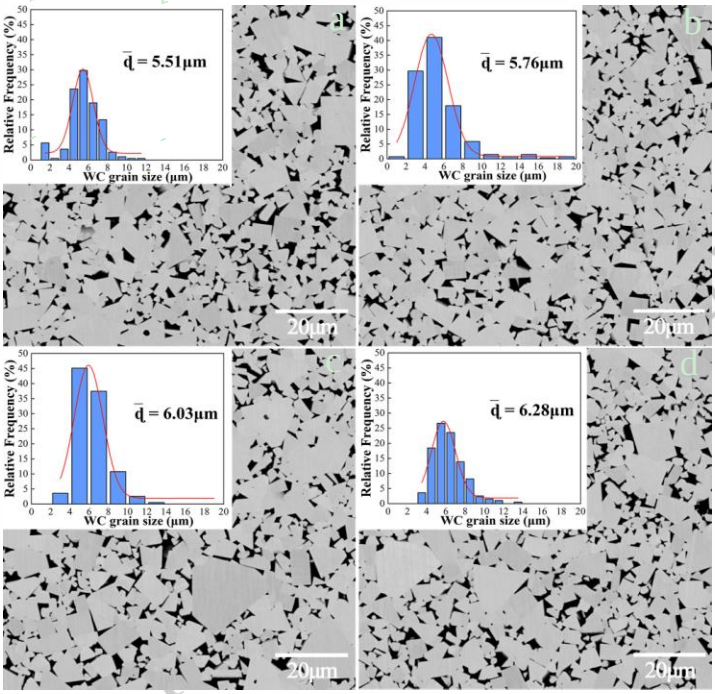

Fig.4 SEM images of ultra-coarse WC-8(Co,Ni) cemented carbides with different Ni:Co ratios: (a) N00 (b) N02 (c) N04 (d) N06

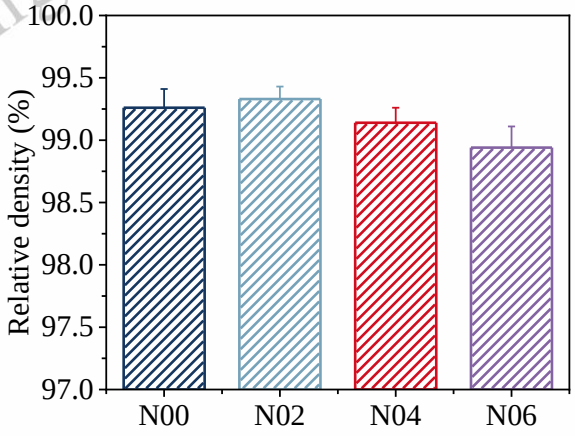

Fig.5 The relative density of ultra-coarse WC-8(Co,Ni) cemented carbides with different Ni:Co ratios.

2.2 Mechanical properties

Fig. 6 presents the Vickers hardness and fracture toughness of ultra-coarse WC-8(Co,Ni) cemented carbides with varying Ni:Co ratios. The Vickers hardness consistently decreases with increasing Ni:Co ratio. Based on the Hall-Petch equation and its relationship with hardness, it is known that finer WC grains possess higher grain boundary strength[18]. The increase of the Ni:Co ratio from 0:8 to 6:6 results in a reduction of the alloy's Vickers hardness. It is noteworthy that the addition of Ni from 0 to 2 wt.% in the N02 alloy does not lead to a significant decline in hardness. This phenomenon may be attributed to the fact that the solid-solution strengthening mechanism introduced by Ni in Co increases the dislocation resistance and impedes the substantial reduction in hardness. For ultra-coarse cemented carbides, there exists an inverse relationship between hardness and fracture toughness[19]. Consequently, the fracture toughness of the alloy increases from 20.75 Mpa $m^{1/2}$ to 22.06 Mpa $m^{1/2}$. Some studies suggest that the dissolution of Ni in Co effectively hinders the transformation of fcc-Co to hcp-Co, which possesses a greater number of slip systems. Dislocations in fcc-Co are more prone to slip when external loads are present, resulting in higher fracture toughness.

Fig. 7 presents the flexural strength of ultra-coarse WC-8(Co,Ni) cemented carbides with varying Ni:Co ratios. As observed in Fig., the flexural strength of the alloy initially rises, but then experiences a significant decrease as the Ni content within the binding phase increases. At a Ni:Co ratio of 4:4, the N04 alloy exhibits the highest flexural strength, reaching 2518 MPa. This phenomenon can be attributed to the distinct atomic radii of Ni and Co. An elevated Ni content results in considerable lattice distortion, increasing the resistance to dislocation motion. In addition, the solid-solution strengthening contributes to the enhanced flexural strength[20]. Moreover, a minor amount of Ni promotes the densification of the alloy, reducing internal defects such as crack sources and micro-porosities, further enhancing the flexural strength. Pre-

vious research has confirmed that the strength of the binder phase (WC/binder) in cemented carbides is higher than that of WC/WC [21]. Therefore, the increase in Ni content within the binding phase also leads to the enlargement and coarsening of WC grains, resulting in localized aggregation of the binder phase and mutual contact between WC grains. This, in turn, reduces the contact area between the WC and the binder phases, leading to a reduction in the localization strength and making the alloy susceptible to crack initiation under external loads, ultimately leading to a significant reduction in the flexural strength.

Fig. 8 presents SEM images of sample fracture surfaces, aiming to further analyze the trends in flexural strength variation with respect to the Ni:Co ratio. From these images, it becomes evident that WC grains exhibit a polygonal shape and are enveloped by the white fractured binder phase[22]. In Fig. 7a, WC grain distribution appears uniform, with well-defined edges and minimal clustering. The primary fracture modes observed are transgranular fractures, along with a few instances of intergranular fractures. In Fig. 8b, it is apparent that in the N02 alloy, the distribution of the binder phase and WC grains is even more uniform, with a scarcity of observed defects such as pores. This indicates that the addition of a small amount of Ni does not significantly impact the microstructure. Moreover, there is an increase in the occurrence of intergranular fractures. Since intergranular fractures consume more energy during the fracture process, the flexural strength of the alloy increases. However, both Fig. 7c and Fig. 7d reveal the presence of abnormally large grains and a significant aggregation of WC grains. Particularly in the N06 alloy, a substantial number of pores are detected. As pores are the primary sources of cracks in the alloy, they lead to the concentration of internal stresses and eventual cracking under external forces, resulting in a significant reduction in flexural strength.

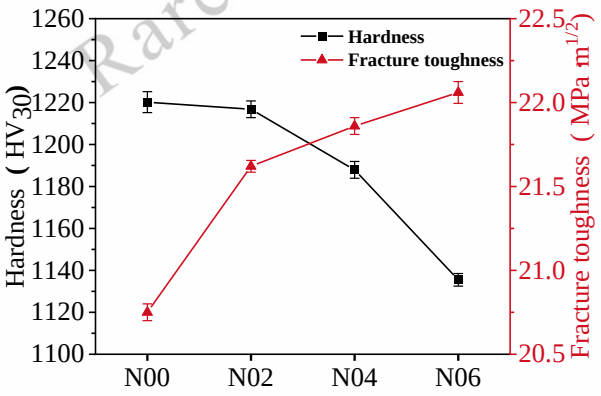

Fig.6 The Vickers hardness and fracture toughness of ultra-coarse WC-8(Co,Ni) cemented carbides with different Ni:Co ratios

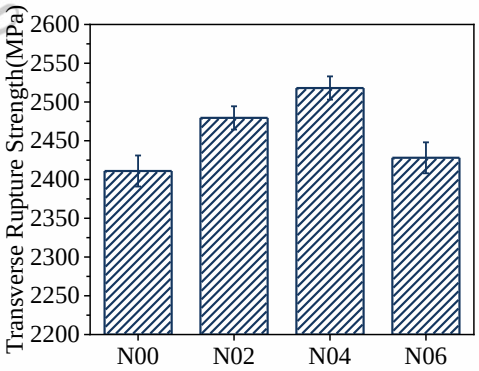

Fig.7 The flexural strength of ultra-coarse WC-8(Co,Ni) cemented carbides with different Ni:Co ratios

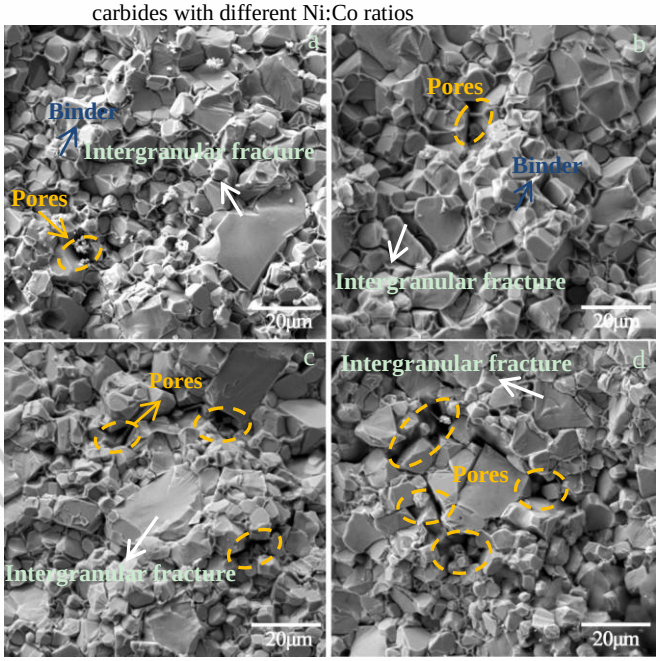

Fig.8 The fracture surfaces of ultra-coarse WC-8(Co,Ni) cemented carbides with different Ni:Co ratios: (a) N00 (b) N02 (c) N04 (d) N06

2.3 Corrosion behaviors

Fig. 9 illustrates the polarization curves and Nyquist plots for ultra-coarse WC-8(Co,Ni) cemented carbides with varying Ni:Co ratios when immersed in a 3.6 wt.% NaCl solution. Table 1 summarizes the corrosion-related parameters obtained through fitting. It is clear that the trends in the polarization curves of the alloys are fundamentally consistent. As the Ni:Co ratio in the binding phase increases, the corrosion potential (E_{corr}) of the alloy continuously shifts toward a more positive direction, the corrosion current density (I_{corr}) gradually decreases, and the impedance values consistently increase. This suggests that increasing the Ni content in the bound phase effectively enhances the corrosion resistance of the alloy. The dissociation of Co and Ni occurs at the anode during electrical polarization due to the sharp difference in electrode potential between WC and Co/Ni. At this point, due to the lower standard electrode potential, Co is more susceptible to oxidation reactions, and therefore, alloys with higher Ni con-

tent exhibit greater corrosion resistance. In addition, as Ni coarsens the WC grains, it reduces the contact area between the bound phase and the caustic solution, thus reducing the corrosion rate of the alloy surface[23]. It is worth noting that, in comparison to the N02 alloy, the reduction in the corrosion current density for N04 and N06 alloys is not significant. This is because, with Ni:Co ratios exceeding 2:6, the presence of increased porosity and microcracks in the alloy leads to a larger contact area between the alloy's surface and the corrosive liquid, thereby weakening the corrosion resistance enhancement mechanism of Ni.

Fig. 10 presents SEM images of the corrosion surfaces of the alloy along with localized EDS analysis. The images clearly reveal distinct variations in the morphology of the corroded surface of the alloy. In Fig. 10a, numerous corrosion pits are observed on the alloy surface with WC grains exposed. This indicates that the binding phase has undergone varying degrees of corrosion dissolution. As the Ni content in the binding phase increases, the number of corrosion pits on the alloy gradually decreases. Additionally, local EDS results indicate an increasing presence of Co and Ni. This suggests that the dissolution of the Co-Ni binding phase within the alloy gradually diminishes, providing further evidence that increasing the Ni content in the binding phase effectively enhances the corrosion resistance of the alloy.

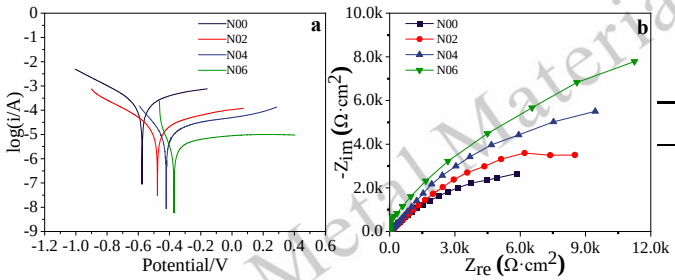

Fig.9 Ultra-coarse WC-8(Co,Ni) cemented carbides in NaCl solution: (a) Potentiodynamic polarization curves (b) Nyquist plots

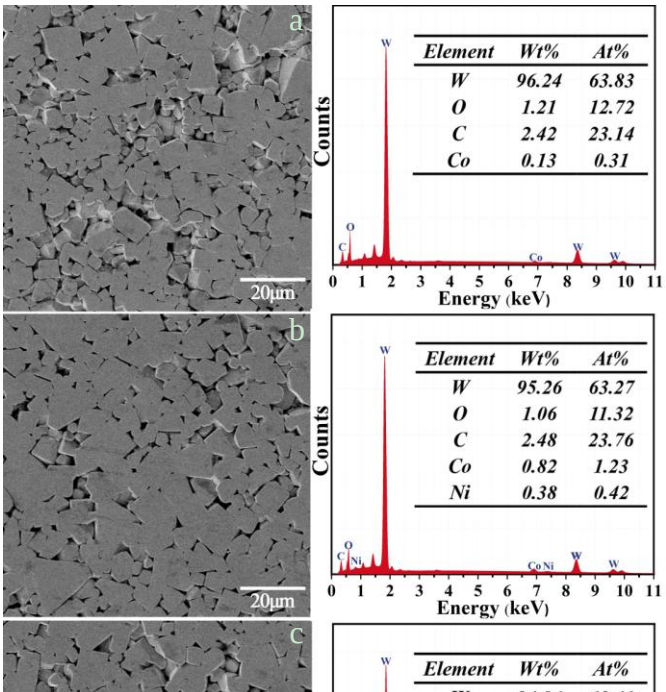

Fig.10 Typical SEM micrographs showing the corroded surface of ultra-coarse WC-8(Co,Ni) cemented carbides and their corresponding EDS analyzation results: (a) N00 (b) N02 (c) N04 (d) N06

Table 1 Electrochemical corrosion data of the four alloys in neutral NaCl solution

Material	E_{corr}(mv)	I_{corr}(μA/cm^2)	Rct(Ω·cm^2)
N00	-587	30.67	8873
N02	-486	13.73	10812
N04	-412	7.65	12755
N06	-373	5.35	13946

3 Conclusions

1) Based on thermodynamic phase diagram calculations, carbon supplementation during the preparation of cemented carbides effectively prevents the occurrence of defects such as decarburization and carbide infiltration in ultra-coarse WC-8(Co, Ni) cemented carbides.

2) With an increase in the Ni:Co ratio in the binder phase, the relative density of the alloy initially increases and then decreases. As the WC grain size increases, the distribution of the binder phase becomes inhomogeneous. The Vickers hardness continuously decreases, while the fracture toughness increases. The bending strength shows an initial increase followed by a significant decrease. When the Ni:Co ratio is 2:6, the alloy exhibits a uniform microstructure and better overall mechanical properties.

3) Using a 3.6wt.% NaCl solution to simulate seawater, the corrosion resistance of ultra-coarse WC-8(Co, Ni) cemented

carbides gradually improves with an increasing Ni content in the binder phase. However, when the Ni:Co ratio exceeds 2:6, the corrosion resistance of the alloy is limited due to the effect of defects such as pores.

References

1 WangLi,Yuan Min,Li Yi et al.*Rare Metal Materials and Engineering*[J],2020,49(12):4016-4022

2 Gao Yang,Luo Binghui,Bai Zhenhai.*Rare Metal Materials and Engineering*[J],2020,49(3):0842-848

3 Wei Su,Zhu Huang,Xingrun Ren et al.*International Journal of Refractory Metals and Hard Materials*[J],2016,56:110-117

4 Tang Yanyuan,Zhong Zhiqiang,Chen Bangming et al.*Rare Metal Materials and Engineering*[J],2023,52(8):2805-06 (in Chinese)

5 Songbai Yu,Fanlu Min,Guobing Ying *et al*.*International Journal of Refractory Metals and Hard Materials*[J],2021,180:111386

6 W.D.Schubert,R.Steinlechner,R.de Oro Calderon.I*nternational Journal of Refractory Metals and Hard Materials*[J],2023,116(11):106346

7 Yang Gao,BingHui Luo,Kejian He et al.*Ceramics International*[J],2018,44(2):2030-2041

8 Chenhao Zhao,Shubo XU,Hui LI et al.*Rare Metal Materials and Engineering*[J],2023,52(10):3547-3555

9 J. Jayaraj,Mikael Olsson.*International Journal of Materials Research*[J],2021,100:105621

10 Zhihao Tian,Yingbiao Peng,Lianwu Yan et al.*Rare Metal Materials and Engineering*[J],2021,50(1):229-234 (in Chinese)

11 X.Q. Han,N. Lin,X.C. Zhang et al.*Journal of Alloys and Compounds*[J],2023,947(6):169603

12 P. Pereira a b,L.M. Vilhena c,J. Sacramento b d et al.*Wear*[J],2021,482-483(10):202924

13 Hongjin Zhao,Luo Wuyi Shen,Haixia Tian et al.*International Journal of Materials Research*[J],2022,113(10):900-910

14 Xuemei Liu,Zhantao Liang,Haibin Wang et al.*International Journal of Refractory Metals and Hard Materials*[J],2022,105:105827

15 X.Q. Han,N. Lin,X.C. Zhang et al.*Journal of Alloys and Compounds*[J],2023,947:169603

16 Tao Lin,Qianghua Li,Yu Hanet al.*International Journal of Materials Research*[J],2022,103:105782

17 Xiang Zhang, Jianhua Zhou, Chao Liu et al.*International Journal of Materials Research*[J],2019,80:123-129

18 Aniss-Rabah Boukantar,Boubekeur Djerdjare,Fernando Guiberteau et al.*International Journal of Materials Research*[J],2021,95:105452

19 Shiwei Li,Zhaoxi Li,Yipeng Chen et al.*International Journal of Refractory Metals and Hard Materials*[J],2022,103:105736

20 Yang Gao, BingHui Luo, Kejian He et al.*Vacuum*[J],2022,30:103081

21 Xiao Hui Yang,Kai Fei Wang,Kuo Chih Chou et al.*Materials Today Communications*[J],2020,49(3):0842-848

22 A.J. Gant,J.W. Nunn,M.G. Gee et al.*Wear*[J],2017,376-377 A(4):2-14

23 Zhenyun Lu,Jin Du,Yujing Sun et al.*International Journal of Refractory Metals and Hard Materials*[J],2021,97(6):105516

基于热力学相图计算开发不同 Ni:Co 比率的超粗晶 WC-8(Co,Ni)硬质合金

商志伟[1]，孙志平[1,2]，王致明[1,2]，赵文凯[1]，陈雅宁[1]

(1.机械工程学部齐鲁工业大学，山东济南 250353)

(2.山东省机械设计研究院，山东济南 250353)

摘要：本研究基于热力学相图计算，利用粉末冶金工艺制备不同 Ni:Co 比率的超粗晶 WC-8(Co,Ni)硬质合金，研究了合金的微观结构、力学性能及其腐蚀性为。结果表明，通过热力学计算相图控制碳平衡，有效避免合金中出现缺碳与富碳的有害相。随着 Ni:Co 比率增加，合金的致密性先增大后减少，WC 平均晶粒尺寸增大，并使得粘结相分布均匀性变差，硬度降低，断裂韧性升高，抗弯强度先升高后大幅降低。Ni 有效缓解了粘结相的腐蚀速率，增强了超粗晶硬质合金的耐蚀性能。当 Ni:Co 比率为 2:6 时，合金的综合力学性能最佳，耐蚀性增强效果明显。

关键词：超粗晶硬质合金; Ni添加;相图;性能; 耐蚀性

作者简介：商志伟，男，1997 年生，硕士生，山东齐鲁工业大学机械工学部，山东济南 205353，E-mail:szw681188@163.com